

# Dynamic changes in traction forces with DC electric field in osteoblast-like cells

Sami Curtze<sup>1</sup>, Micah Dembo<sup>2</sup>, Miguel Miron<sup>1</sup> and David B. Jones<sup>1,\*</sup>

<sup>1</sup>Department of Experimental Orthopedics and Biomechanics, Philipps-University Marburg, Baldingerstr., 35033 Marburg, Germany

<sup>2</sup>Department of Biomedical Engineering, Boston University, 44 Cummington Street, Boston, MA 02215, USA

\*Author for correspondence (e-mail: jones@post.med.uni-marburg.de)

Accepted 23 January 2004

Journal of Cell Science 117, 2721-2729 Published by The Company of Biologists 2004

doi:10.1242/jcs.01119

## Summary

**Primary bovine osteoblasts and human osteosarcoma cells exposed to direct-current electric fields undergo processes of retraction and elongation ultimately resulting in the realignment of the long cellular axis perpendicular to the electric field. The time taken for this reorientation was inversely correlated to field strength within a certain range. Cellular force output during reorientation was analyzed using a simple modification of traction force microscopy. The first detectable reaction was an increase in average traction force magnitude occurring between 10 and 30 seconds of electric field exposure. In the following 2 to 15**

**minutes traction forces at margins tangential to the electric field decreased below their initial values. Phase-contrast microscopy revealed elongating protrusions at these margins several minutes later. We could not correlate the initial traction changes with any change in intracellular free calcium levels measured using the fluorescent dye Fura-2 AM.**

Key words: Traction-force imaging, DC electric fields, Cell orientation, Osteoblasts

## Introduction

Alignment due to direct-current (DC) electric field exposure has been observed in a variety of cells (Cooper and Keller, 1984; Onuma and Hui, 1988; Harris et al., 1990; Nuccitelli and Erickson, 1983). In this alignment process cells usually retract the lamellae oriented parallel to the electric field gradient and extend those oriented perpendicularly. In addition to alignment, cells migrate in electric fields according to various characteristic patterns. For example, fish epidermal keratocytes move towards the cathode (Cooper and Schliwa, 1985) and embryonic spinal neurites from *Xenopus laevis* move towards both electrodes (Stewart et al., 1995).

How cells sense the direction of the field and the mechanisms underlying the migration and orientation remain largely unknown. For instance, it is not known whether the electric field is sensed through a direct force acting on the whole cell or, more likely, if the electric field disrupts a cellular structure, such as a receptor. Another possibility is that the electric field modifies a cellular biochemical process causing the cell to undergo an active orientation process. In addition, there is little understanding of the signal transduction pathways that convert the initial signal into the large cytoskeletal reorganizations and shape changes that occur later. A role for intracellular calcium in this signaling process is suggested from data showing a delayed increase of intracellular  $\text{Ca}^{2+}$  after application of a DC field (Onuma and Hui, 1988; Cooper and Schliwa, 1985). It is proposed that the initial withdrawal of the protrusions from the electrode-facing cell margins is in response to the transmembrane potential disruption and subsequent opening of calcium channels (Cooper and Keller, 1984; Cooper and Schliwa, 1985). Intracellular  $\text{Ca}^{2+}$  changes can lead to dramatic structural cytoskeleton remodeling and

changes in contractile forces (Forscher, 1989; Strohmeier and Bereiter-Hahn, 1984; Rees et al., 1989). Cellular traction seems to be a very early target of the signaling pathway. Embryonic chick fibroblasts cultivated on silicon rubber substrates react quickly to a DC field (within five minutes) shown by a slight weakening of traction on cell margins facing the electrodes (Harris et al., 1990) before major cytoskeletal rearrangements are observed.

Some of the many theories of electro-reception propose a mechanical effect. Indeed responses to electric fields like the dynamic changes in intracellular free calcium, traction and orientation are similar to the response cells undergo after mechanical stimulation. In this investigation we used primary bovine osteoblasts (POBs) and an osteoblast-like osteosarcoma cell line, MG63. POBs produce significantly higher traction forces than fibroblasts and MG63 cells (total forces of 660 nN/cell compared to 50 nN) and are also much more mechano-sensitive than fibroblasts (Jones et al., 1991). MG63 cells are equally as sensitive to mechanical deformations as POBs but have a significant advantage in being far easier to transfect, for instance with actin-GFP fusion constructs. To apply distinct DC electric fields to these cells without unwanted effects like electrolysis, electro-osmosis or joule heating, we developed an electro-chamber based on the model of Harris et al. (Harris et al., 1990). Cells were exposed to fields between 5 and 12 V/cm. In our experiments it was evident that both primary bovine osteoblasts and MG63 human osteosarcoma cells were sensitive to very low electric fields. Both these cell types, like fibroblasts, react with alignment and elongation perpendicular to the polarity of a DC electric field.

Using these very sensitive cells we studied the dynamics and sequence of the orientation reaction to discriminate between

the different underlying mechanisms. The cellular force output after field application was determined using collagen-coated flexible polyacrylamide substrates and the traction force was measured using a reported method (Dembo et al., 1996), with slight improvements as described (Dembo and Wang, 1999; Munevar et al., 2001). This method uses Bayesian computation to calculate the maximum traction forces likely for pre-assigned nodes within the cell boundary with high temporal and spatial resolution. We introduce here a further simple modification to visualize very small changes in traction force over a few seconds by calculating the differential force between two time-points.

Cells elongated in the same direction as the polarity of the electric field initially increase their traction forces within 30 seconds and then retract. Subsequently these cells relax slightly along the margins parallel to the polarity of the electric field. At these margins new protrusions are formed, leading to elongation along an axis perpendicular to the polarity of the electric field. The role of intracellular  $\text{Ca}^{2+}$  during the orientation process was studied with the Fura-2 ratio method (Grynkiewicz et al., 1985). Intracellular  $\text{Ca}^{2+}$  changes were recorded, but only after 90 seconds, suggesting that calcium might not be responsible for the early signaling events. Morphological changes were detectable after about 5 minutes.

## Materials and Methods

Osteoblasts were prepared using an outgrowth method (Jones and Bingmann, 1991). The preparation of periosteum pieces of bovine ulnae and steer radii obtained at the local slaughterhouse led to a homogeneous culture of osteoblast-like cells after 3 to 5 weeks. The cells were cultured in HIGEM (BioWhittaker, Germany) containing 10% FCS (Seromed, Lot S0112/511S, Germany). The outgrowing osteoblasts reached confluence and were harvested using collagenase and Tyrode's solution. MG63 osteosarcoma cells (Billiau et al., 1977) were obtained from the ATCC USA and cultured in RPMI 1640 (Sigma, Germany). The cells were cultured on cover slips (No. 1, 60×24 mm; Marienfeld, Germany) or on collagen-coated polyacrylamide gels at a density of 3000 cells/cm<sup>2</sup>. For the experiments, cover slips were mounted into an electro-chamber filled with 10 mM HEPES Ham's F10 medium (PAA Laboratories, Austria).

We developed an electro-chamber based on the model of Harris and colleagues (Harris et al., 1990). The chamber has two containers, one at each side, these are filled with 0.9% saline solution and the electrical current is introduced using platinum wires. For application of the electric field to the cells, we used agar bridges; one end was placed in the container and the other end at the side of the cell chamber. Agar bridges permit the flow of current but block convection of toxic substances from the wires (Jorgensen, 1972), electrolysis and electro-osmosis (Steckel et al., 1984), as well as joule heating (Brighton et al., 1975). In the middle of the chamber there is a block of polycarbonate, which serves to insulate the two margins of the cover slip where the agar bridges are placed. The block also produces a high surface-area-to-volume ratio for heat transfer and confines the electric current to a 100- $\mu\text{m}$ -thin strip of culture medium between the cells and the bottom of the block.

A platinum wire is attached to both sides of the block, this is connected to a multimeter (Fluke 75, Fotronic Corporation, Melrose, MA) for controlling the field strength generated by a power supply (Biorad 200/2.0 voltage-regulated, Life Science, Hercules, CA).

Infrared measurements were used to check the temperature under the bridge. With fields up to 15 V/cm no significant increase in temperature was detectable. After 24 hours with no electric field the cells looked normal and arranged themselves with random orientations.

Intracellular calcium concentration was measured with the Fura-2 ratio imaging method. Briefly, cells on cover slips were loaded with 3  $\mu\text{M}$  fura-2/acetoxymethyl ester (Fura-2 AM, Molecular Probes, The Netherlands) for 60 minutes at room temperature. After loading, cells were washed twice with PBS and then mounted into the electro-chamber with 10 mM HEPES medium. Sequential 1 second, 512×512 8-bit 340/380 excitation images were gained with an intensified CCD camera (Extended ISIS, Photonic Science, UK), controlled by a monochromator (Visitech, Sunderland, UK) and were processed using a Quanticell 700 (Applied Imaging-Visitech, Sunderland, UK). The camera was attached to a Nikon Diaphot IM microscope using a Nikon 40×, n.a. 0.85 fluorescence objective. Fluorescence emission was collected from a group of three to five cells. Excitation wavelength was alternated between 340 nm and 380 nm and fluorescence intensity ( $F_{340}$  and  $F_{380}$  respectively) was monitored at 505 nm. Calcium concentration was indicated by the  $F_{340/380}$  ratio (Grynkiewicz et al., 1985).

The motility of osteoblasts during electric field application was examined using a 40×, n.a. 0.60 objective (Leitz, Germany) on a Diavert inverted microscope (Leitz, Germany). Cell responses and traction force images were documented using a CCD camera (Xillix microImager M1400). Fluorescence microscopy combined with phase-contrast imaging was carried out on a Nikon Diaphot IM microscope (as above).

The method for preparing thin collagen-coated polyacrylamide sheets has been previously described (Wang and Pelham, 1998; Dembo and Wang, 1999). The substrates were 8% acrylamide and 0.04% or 0.06% bis-acrylamide containing 2% of a 1:1 mixture of 0.2  $\mu\text{m}$  and 0.5  $\mu\text{m}$  fluorescent latex-bead dilutions (FluoSphere, Molecular Probes, Leiden, The Netherlands). A 14- $\mu\text{l}$  volume of this solution was used for substrates covered with circular cover slips (No. 1, 16 mm diameter, Marienfeld, Germany). Cover slips were coated with type-I collagen as described by Wang and Pelham (1998).

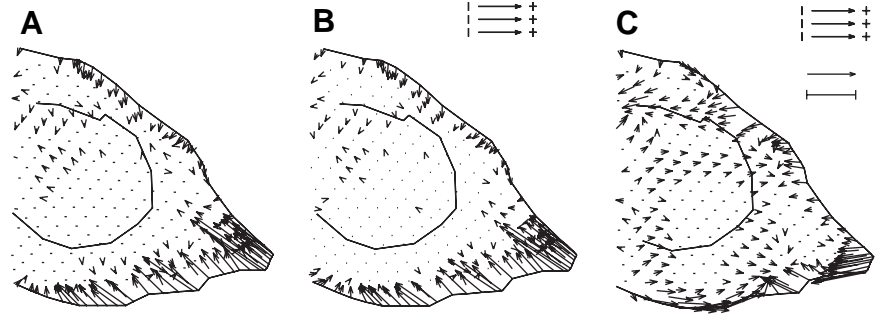
A method based on the Hertz theory (Radmacher et al., 1992) was used to determine the flexibility of the polyacrylamide substrata. An atomic-force microscope (AFM) with a small ball at the top of the cantilever as described previously (Struckmeier et al., 2001) was used to press on the polyacrylamide sheets. The total indentation caused by the ball fixed to the cantilever was between 0.5  $\mu\text{m}$  and 1.5  $\mu\text{m}$ . (Maximal displacements caused by the cells are about 1  $\mu\text{m}$  on soft substrates.) We used balls at the tip of the cantilever with a radius between 2 and 10  $\mu\text{m}$ . Young's modulus was calculated as  $Y=3(1-\nu^2)f/4d^{3/2}r^{1/2}$ , where  $f$  is the force exerted on the sheet,  $d$  is the indentation,  $r$  is the radius of the steel ball, and  $\nu$  is the Poisson ratio, which was assumed to be 0.3 (Li et al., 1993). Values for the used sheets are about 4400 N/m<sup>2</sup> (s.d. <1%) for 0.04% and 6800 N/m<sup>2</sup> (s.d. <1%) for 0.06% bis-acrylamide substrates.

The traction forces of the cells were calculated as described (Dembo and Wang, 1999). The cells were cultivated on collagen-coated flexible polyacrylamide sheets containing fluorescent marker beads. The mechanical properties of the gel allow the cell to deform the substratum. The gel relaxes and the marker beads resume their initial position when the cell is removed. Deformations of the substrate were determined as a matrix of vectors, by comparing the fluorescent-light patterns caused by the embedded beads, in the presence and absence of the cell (Marganski et al., 2003). For force calculations we used LIBTRC software from Professor Dembo (Boston, MA) for a Linux platform (Red Hat Linux 7.2).

## Results

To address the question if applying an electric field to a cell causes a change in the traction-force vector map, we calculated differential traction forces by observing the change in substrate displacement, occurring before and after electric field application. This is possible because the cell shape changes

**Fig. 1.** The leading edge of a Mg63 cell on a polyacrylamide substrate ( $Y_M=4320 \text{ N/m}^2$ ). Total traction force in rest (A) and after 30 seconds of electric-field application (B). Differential vectors for the change between A and B are displayed in C. The scale bar represents  $10 \mu\text{m}$ . The scale vector represents  $300 \text{ N/m}^2$  for A and B and  $20 \text{ N/m}^2$  for C.



very slowly which means that over short time periods, changes in displacement and traction are related in a linear fashion. This is different to the approach of most published works on traction where forces are calculated as the difference between one state and the totally relaxed substrate. Here we calculate the small difference between two tensed cellular states occurring over a few seconds. This makes it easier to correlate the reaction of the cell to the applied electric field. The resulting vectors should not be confused with the total traction force generated by the cell. As an example, Fig. 1A shows the total traction force under the leading edge of a cell and Fig. 1B the total force after 30 seconds of electric field exposure at  $10 \text{ V/cm}$ . Calculation of the deformation matrix between Fig. 1A and Fig. 1B gives the differential traction force vectors (see Fig. 1C). Note that the vectors in Fig. 1C are magnified by a factor of 15 compared to Fig. 1A. Thus the differential tractions are only a small fraction of the total traction.

When cells were subjected to DC electric fields of  $10 \text{ V/cm}$ , they aligned and elongated perpendicular to the electric field lines (see Fig. 2). This process took place in two phases; first, cells retracted their lamellar extensions, with the earliest visible retractions between 5 and 10 minutes after the electric field was applied. In the second phase, the cells began to extend perpendicular to the electric field lines. For statistical analysis, a bounding box was drawn around the cells. The  $x$  dimension follows the electric field lines, while  $y$  represents the perpendicular dimension. Fig. 3A,B show these values for one experiment with 17 cells at  $10 \text{ V/cm}$ . Along the electric field lines the cells lost about 46% (12 of  $26 \mu\text{m}$ ) of their length. Perpendicular to the electric field lines they first lost 16% (4 of  $24 \mu\text{m}$ ) in 20 minutes, but then they grew 35% (from  $20 \mu\text{m}$  to  $27 \mu\text{m}$ ) in 100 minutes. The reaction to the electric field especially in this  $y$  direction takes place in two phases: first retraction, then elongation. Fig. 3C shows the ratio of  $x$  and  $y$  as a marker for the orientation. The huge s.d. at the start of the experiment indicates that the cells were elongated but had no preferred orientation. At the end of the experiment most cells had a value lower than one and the s.d. was much smaller, showing that they have one preferred orientation and again

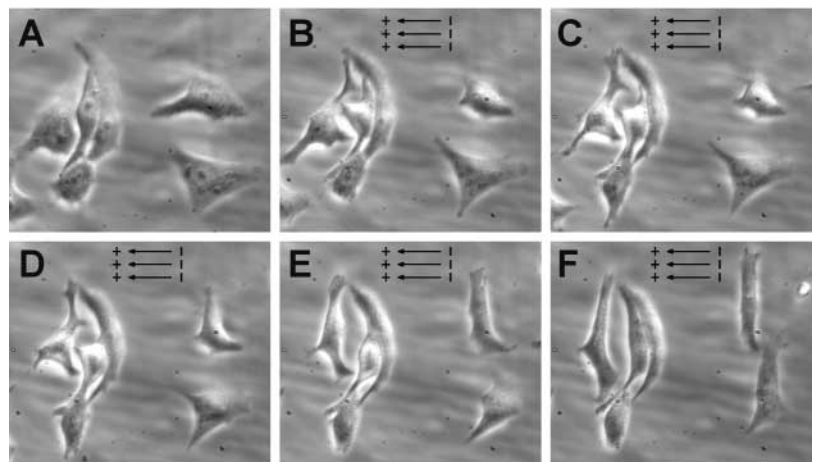
are elongated. The same can be seen in Fig. 3D, where the data from 12 independent experiments at  $10 \text{ V/cm}$  is shown. The average cell has double the value for the  $y$  dimension compared to the  $x$  length along the electric field lines at the end of the experiment. Their major axis was perpendicular to the electric field lines, whereas it was randomly oriented before the experiment. The time for this cellular alignment is inversely correlated to the field strength within a certain range (see Fig. 4). To evaluate if cellular alignment was programmed in the cells after field application, the electric field was turned off after 10, 30 or 60 minutes of application. Cells then spread in all directions, and did not continue their orientation process.

The early retraction phase increased in speed when voltage increased (see Fig. 5). Conversely, with fields greater than  $12 \text{ V/cm}$ , many cells did not elongate. The maximal tolerable time for field exposure is also dependent on field strength. After this time cells did not re-spread as they were dead (see Fig. 4). If cells had not started visible re-spreading within the first 20 minutes after field application had stopped they did not recover at all.

When voltage decreased below  $7 \text{ V/cm}$ , orientation was no longer a two-step process. Whilst retracting very slowly, cells started to spread perpendicular to electric field lines at the same time. The time needed to undergo this process of orientation decreased with the strength of the field (Fig. 4). In summary, osteoblasts respond differently depending upon the strength of the field: with only retraction at high field-strength, with retraction and elongation phases at medium strengths or with simultaneous retraction and elongation at low field-strength.

The cellular responses to electric fields when cultured on polyacrylamide sheets were compared with those carried out on normal glass surfaces. No significant differences were observed.

**Fig. 2.** Phase-contrast light micrographs showing the alignment processes of osteoblasts. Cells were subjected to  $10 \text{ V/cm}$  for 80 minutes. A, cells resting; B, after 30 minutes; C, 60 minutes; D, 100 minutes; E, 150 minutes; and F, 180 minutes of exposure. Signs (+/-) show the polarity of the field.



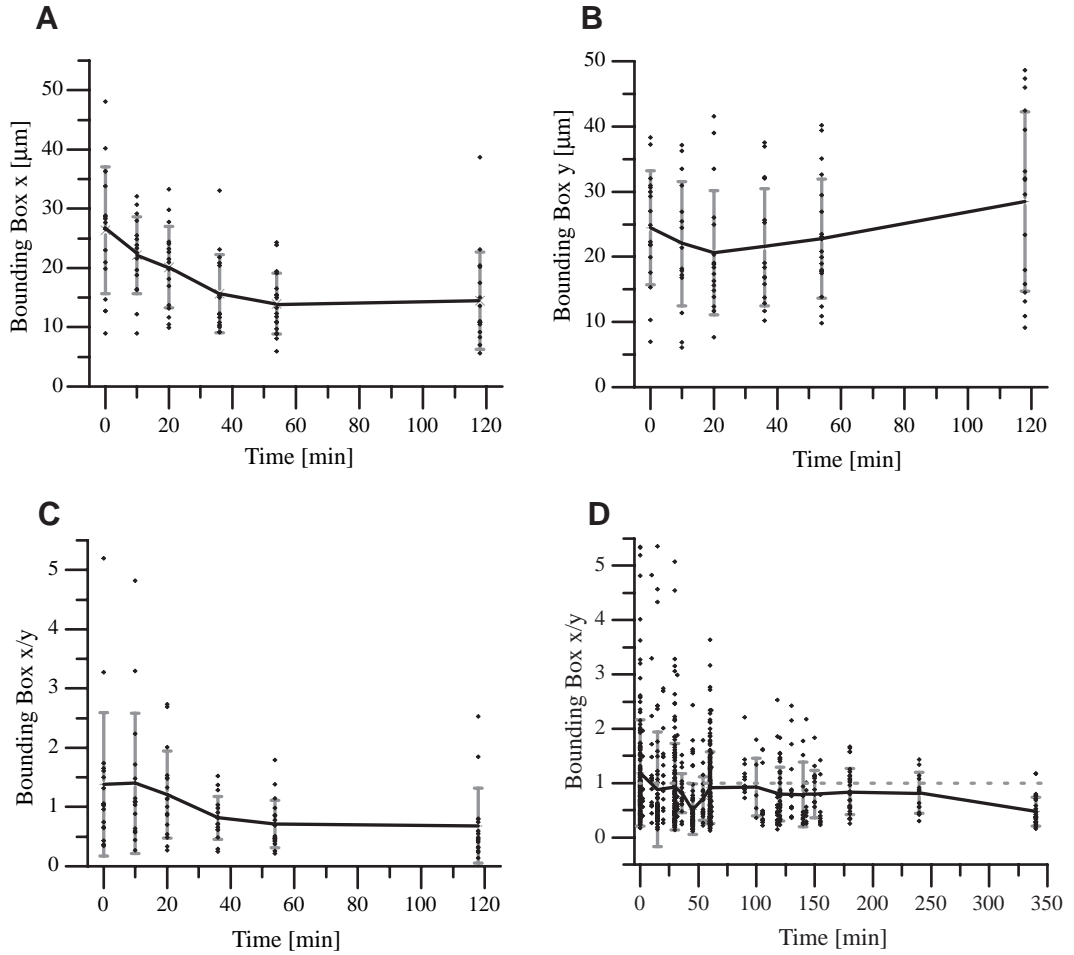
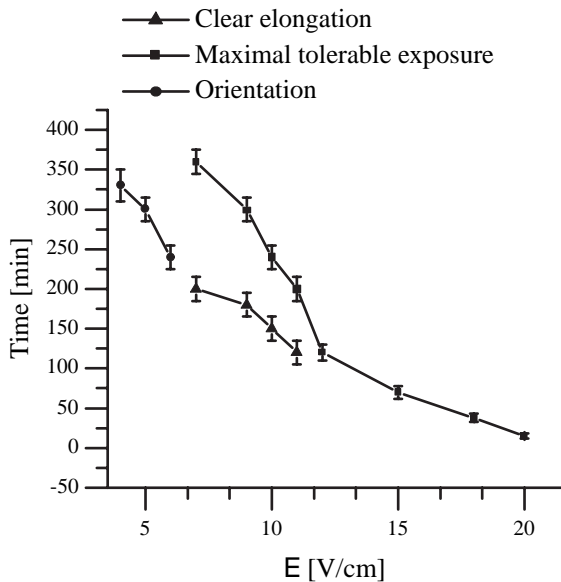


**Fig. 3.** (A) The  $x$  dimension (along the electric field lines) of a bounding box around every cell as a function of the length of time of electric field application at 10 V/cm. (B) The  $y$  dimension (perpendicular to the electric field) of the bounding boxes as in Fig. 3 around every cell as a function of the length of time of electric field application. (C) Ratio ( $x/y$ ) of both sides of the bounding boxes from Fig. 3 and Fig. 4. (D) Ratio ( $x/y$ ) as in Fig. 5, but for all cells from 12 independent experiments with an electric field of 10 V/cm.

To test if the electric field had an effect on the polyacrylamide substrate or the fluorescent beads, the cover slip with the substrate and the embedded fluorescent beads was tested without cells. The experiments with cells were checked by transferring the cell outline coordinates to a cell-free position

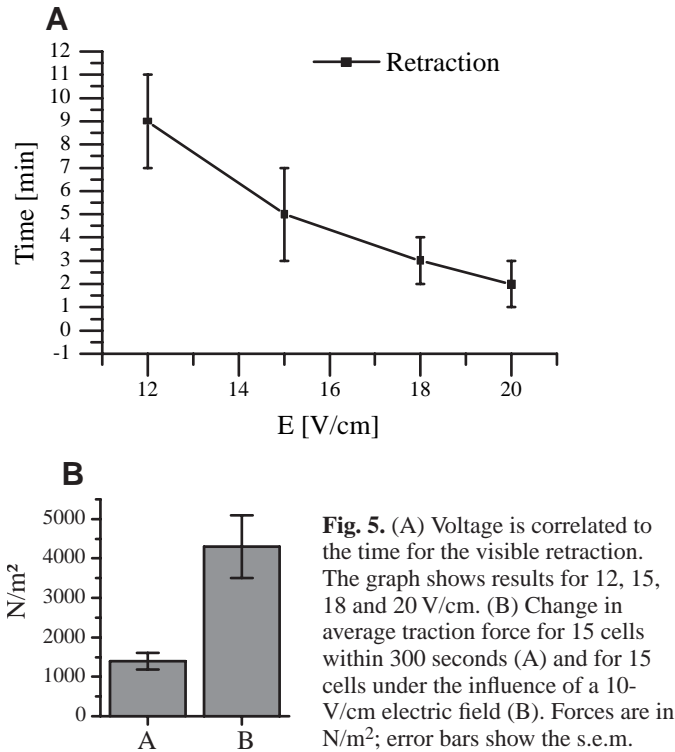
in the field of view. Calculations performed on this field (i.e. without cells) did not produce significant vectors, just random noise. We conclude that the electric field does not have a measurable effect on the polyacrylamide sheets. To check the significance of our observations, cells with and without an electric field were observed for periods of time between 10 and 600 seconds and the differential values for average change in traction force was calculated relative to the zero time point. We observed that differential traction vectors have significantly higher average magnitude when the electric field is present. This shows that the field causes changes larger than spontaneous changes (e.g. changes due to phase of the cell cycle). Fig. 5B shows a difference of 3000 N/m<sup>2</sup> in average differential traction-force magnitude for 0 V and 10 V after 300 seconds.

Fig. 6 shows a representative traction image of an experiment at 10 V/cm. This differential image was computed by comparing the substrate deformation at zero time and after 30 seconds of electric-field application. To visualize the change of the force distribution caused by the electric field, the magnitudes of the differential traction stress at each pixel in the cell area were represented in different colors. Analysis of



**Fig. 4.** The strength of the electric field applied to primary osteoblasts was altered. Time taken for cellular elongation, a clear noticeable orientation and the maximal time under electric-field exposure for cellular re-spreading is shown.





the distribution of the differential-stress magnitudes showed that the largest changes were concentrated to areas in the lamellae where the absolute traction stress was also highest. However, the increase in differential traction force did not occur at all sites where the absolute traction force shows significant vectors. For example, the leading edge of the cell does not necessarily show a significant increase in force. The lowest differential traction forces were found in the middle of the cell, similar to computations of the absolute traction force in a cell. Differential traction patterns correlate with the initial orientation of the cell to the electric field. We found activity close to the periphery and usually the direction of the differential forces was the same as the electric field lines. These findings indicate that the cell is not reorganizing focal contacts and cytoskeletal structures completely in the first minutes after application of an electric field, rather the cell seems to redistribute the force applied to the adhesions. In our experiments, significant differential vectors were observed 30 seconds ( $n=24$ , s.d. 18) after field application. Two cells did not show significant changes due to the electric field. All traction force measurements were performed at 10 V/cm. In 10 experiments images were acquired every 30 seconds, in 14, every 10 seconds. In all 22 cases where the vectors changed significantly, they had a common pattern, of which the one shown in Fig. 6 is representative.

Fig. 7 shows the differential traction forces during an alignment process under field exposure. Different phases of force distribution change can be distinguished before visible changes in cell morphology occur in phase-contrast observation. The first detectable reaction corresponds to an increase in the absolute force of about 5 to 30%. Here the differential vectors all point inwards and are aligned with the absolute traction vectors which generally pull the substrate

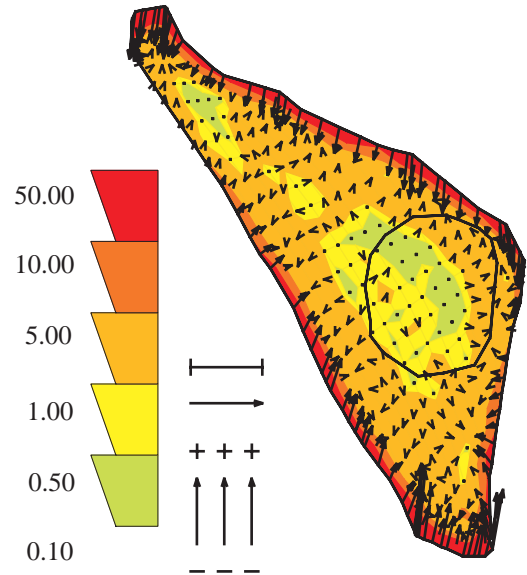


**Fig. 6.** Differential traction forces visualized in pseudocolor according to the intensity and the force vectors in N/m<sup>2</sup>. Traction force changes after an application of a 10-V/cm electric field for 30 seconds on a substrate with a stiffness of 4317 N/m<sup>2</sup> compared to the cell in rest before application are shown. Total traction force is not shown. The vectors show almost the same orientation as the electric field, where +/- labeled scale vectors indicate orientation of the electric field. Scale bar represents 10  $\mu$ m; scale vector represents 50 N/m<sup>2</sup>. Increased inward-pointing traction forces with same orientation as the electric field appear at margins facing the poles.

inwards. This phase starts after 30 seconds but as can be seen from Fig. 8 traction forces keep increasing in the following minutes in some cellular regions.

Vectors at the margins of a cell oriented perpendicular to the electric field lines usually continue to show increased forces in the elongation phase of the alignment reaction, whereas the margins where the cell subsequently elongates show decreased forces. If forces decrease below the baseline before application of the electric field, the direction of the differential vectors change from pointing inwards to outwards as can be seen in Fig. 7F (labeled c, d and e). Here c is typical for the start of retraction where morphological changes are not visible but some cell-to-substrate connections have already been released. The areas labeled d and e have a high probability of producing new visible protrusions in the following minutes. Cellular decrease of force in distinct areas occurs after 90 seconds to 10 minutes (Fig. 7F, d and e). The second phase, where weakening at the margins with the same orientation as the field occurred started on average after 10 minutes but this varied widely. The first cell showed this traction force pattern after 120 seconds whereas one cell took 15 minutes. After the elongation process has taken place, the force starts to increase again at the new elongated protrusions.

We were unable to show a cytoplasmic calcium concentration increase from either intracellular or extracellular sources within the time frame of the first detectable cytoskeletal change in traction force. A mean delay of 85 seconds ( $n=22$ , s.d. 62) between electric field application and first calcium increase occurred. The increase in fluorescence ratio was 31% (s.d. 19). The first measurable increase of intracellular free calcium was

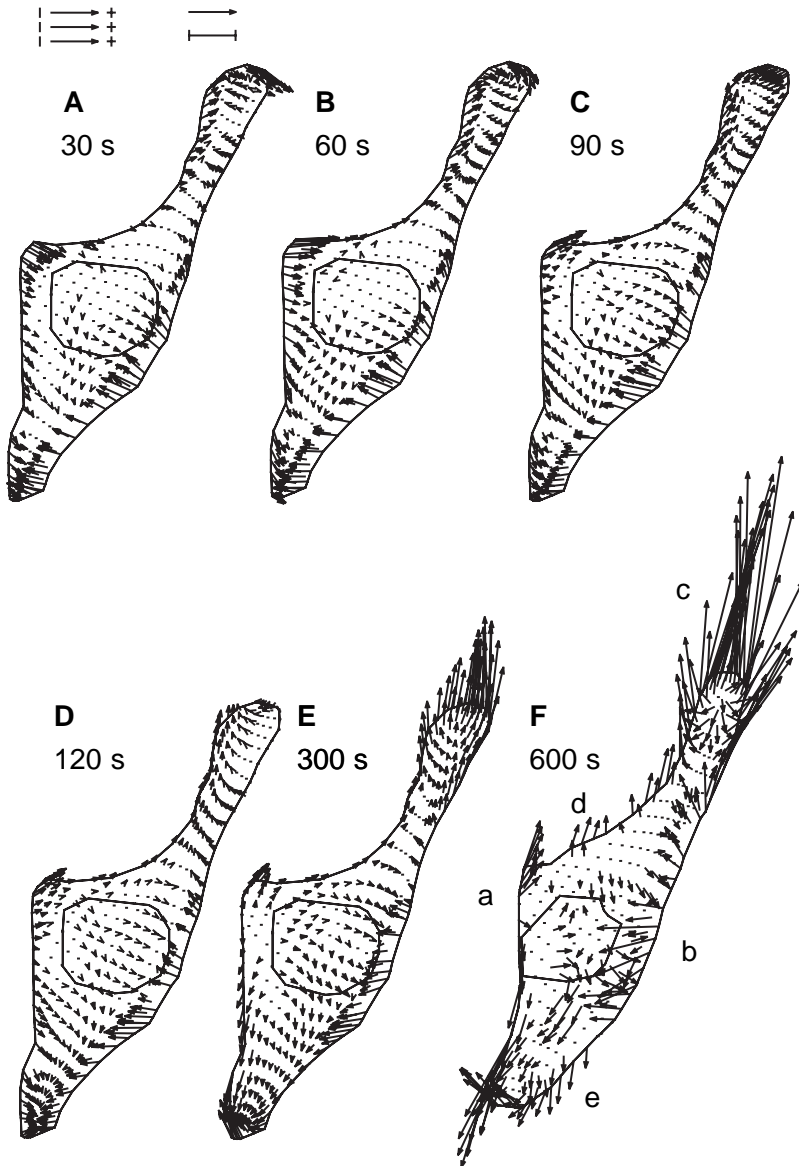


**Fig. 7.** Differential traction forces during cellular alignment as a result of a 10-V/cm electric field in a primary bovine osteoblast on a substrate with a stiffness of 6000 N/m<sup>2</sup>. +/- labeled scale vectors indicate orientation of the electric field. A, the phase of increasing force. After 5 minutes (E and F) the loss of the normally inward-pulling traction forces occur at sides where the cell will start to elongate a few minutes later (d and e). The bar scale represents 10 μm; the scale vector represents 10 N/m<sup>2</sup>. Retraction between E and F is visible at area labeled a and b.

## Discussion

Osteoblasts and MG-63 osteoblast-like osteosarcoma cells react with a cytoskeletal contraction especially of the margins facing the electrodes. One explanation for the resulting elongation normal to the field polarity is that this contraction might lead to a higher cytoplasmic pressure, which causes the cytoplasm to be squeezed to locations of lower resistance, in our case the margins perpendicular to the electric field. In analogy to published work (Bereiter-Hahn and Luers, 1998) we were able to show that cell margins increase cytoskeletal contractility before they retract, and that cytoskeletal contractility decreases at margins where new protrusions occur. Increasing force at margins that are about to be retracted has been reported for locomoting keratocytes analyzed with traction-force measurements performed on wrinkling silicone substrata (Burton et al., 1999). It has been postulated that cells detach from their focal adhesions by increasing traction forces until the attachment disrupts (Jay et al., 1995). This disruption is caused by an increase in ATP and intracellular free calcium concentrations, and is inducible by adding additional ATP (Crowley and Horwitz, 1995). High intracellular calcium transfer occurs in locomoting cells just before detachment of the rear of the cell, and increasing calcium levels using ionophore A23187 or IP<sub>3</sub> leads to a retraction of the rear of the cell (Lee et al., 1999). So an

increment of pulling traction forces occurring after application of a DC electric field might lead to a disruption of contacts to the substrate, which leads to a visible retraction. In other experiments we were able to show that cells do not react to electric fields if substances that block calcium channels like nifedipine, cadmium or lanthanum are applied (manuscript in preparation). This also occurs 20 minutes after thapsigargin is used, indicating that both calcium channels and intracellular free calcium from IP<sub>3</sub>-sensitive intracellular Ca<sup>2+</sup> stores are needed for the retraction process. This possibly occurs by several mechanisms; the most important of which causes the detachment of focal adhesions.

The first morphological changes caused by electric fields were detected within 30 seconds in rat prostate cancer cells (Djamgoz et al., 2001). However, we found the first changes after 5 minutes but the first increase of cytoskeletal contractility after just 10 seconds and a mean delay of 85 seconds for Ca<sup>2+</sup> changes. We could not find a correlation between changes in intracellular free calcium and the initial contraction, which

after 17 seconds. Fig. 9 shows an example of an experiment where the calcium response of 6 cells to a 10-V electric field was measured. One cell reacted within 34 seconds, but the mean time to reaction was 78 seconds.

In the range 7 to 12 V/cm both primary osteoblasts and MG63 react in essentially identical ways. The first detectable reaction was an increase of 5-30% in the inward-acting traction forces within 30 seconds. The principle vector of the force increase is parallel to the field vector, which indicates a direct sensing of the field. Before any observable cell movement, between 2 and 15 minutes, there is a distinct weakening at margins parallel to the electric field lines. The visible retraction phase starts after 5 to 10 minutes. The delay of onset of this process decreases with voltage. Cells subsequently elongate perpendicular to the electric field. The elongation process is negatively correlated to field strength. For fields of less than 7 V/cm the retraction phase is so slow that the visible elongation starts during the retraction phase, so that just an orientation process is visible.

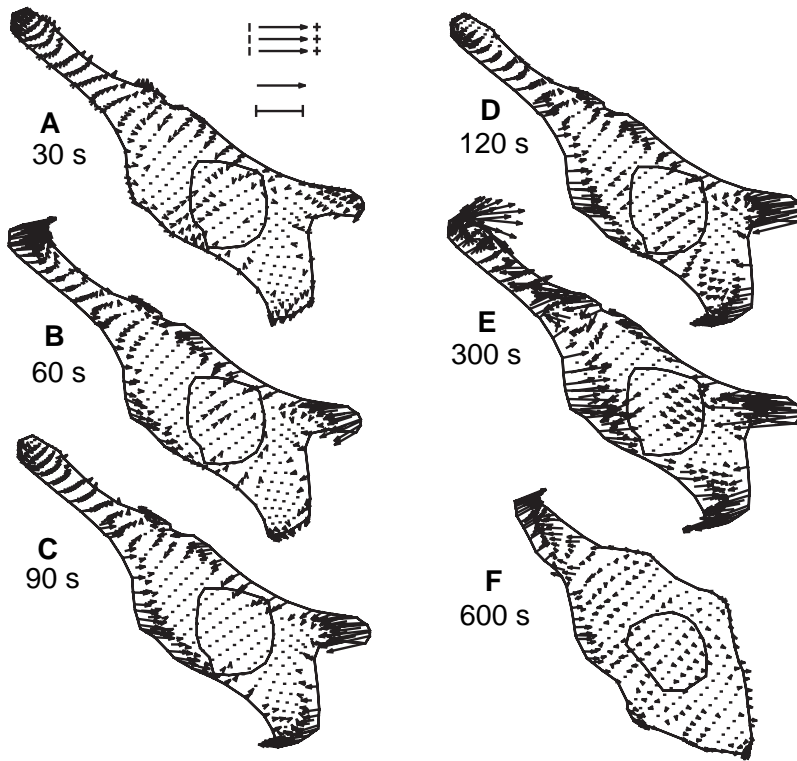


**Fig. 8.** Differential traction forces during cellular alignment in a 10-V/cm electric field in a MG63 cell on a substrate with a stiffness of 4000 N/m<sup>2</sup>. +/- labeled scale vectors indicate orientation of the electric field. Traction forces increase in some cellular regions up to the 300th second. Scale bar represents 10  $\mu$ m; scale vector represents 10 N/m<sup>2</sup> for A to E and 50 N/m<sup>2</sup> for F.

suggests that the initial sensing of the field vector and the first mechanical responses is independent of Ca<sup>2+</sup> concentration. There is evidence that electric-field-directed fibroblast locomotion and galvanotropism of *Xenopus* spinal neurites is Ca<sup>2+</sup> independent (Brown and Loew, 1994; Palmer et al., 2000).

However, there appears to be a strong similarity in many of the responses to electric fields, cell movement and mechanical stimulation of the cell. Stretch-activated calcium channels may be responsible for calcium influx in regions of applied mechanical forces (Glogauer et al., 1997), this then leads to a stiffening of the cytoskeleton in the region of the applied force mainly by actin polymerization. Different models of sensing the mechanical signal over contacts with the extracellular matrix have been postulated. The existence of a strain sensor at transmembrane linkages that produces biochemical signals to modulate cell reactions has been suggested (Sheetz et al., 1998). In this position a sensor can react to external stimuli conducted via integrins and at the same time they can sense cytoskeletal forces transmitted to these integrins. One candidate for this, because of its association with integrins is the focal adhesion kinase (FAK). FAK is known to be involved in mechanosensing during fibroblast migration (Wang et al., 2001) as well as in mechanosensing of osteoblasts (Moalli et al., 2001).

Perpendicular orientation to a mechanical-force axis can be seen in osteoblasts that are cyclically stretched by more than 4% of their length (Neidlinger-Wilke et al., 2001). This can also be explained by supposing that the stretch in the long axis disturbs the cells more than in the perpendicular one, or that cyclic strain leads to an increased probability of disrupting contacts to the extracellular matrix connected to tensed actin fibers. Upon constant strain, skeletal muscle cells align parallel to the deformation axis (Collinsworth et al., 2000). XTH-2 and 3T3 cells elongate protrusions and move towards a constant-

strain stimulus when cultivated on flexible substrates (Lo et al., 2000; Karl and Bereiter-Hahn, 1999).

Strongly related to mechanosensing is durotaxis, where an orientation of the cell occurs that is similar to that for cells under the influence of electric fields. The term durotaxis was proposed for a cellular reaction where cells on a gradient substrate prefer to move to the stiffer side (Lo et al., 2000). Cells are easily able to move from the soft to the stiff side, but if a cell approaches the soft substrate from the stiff side, the cells stop crawling and producing new lamellipodia in the direction of the leading edge. While the retraction at the tail continues, cells start to spread parallel to the border between soft and stiff side, remaining on the stiffer side. This way the cells become orientated perpendicular to the gradient of elasticity for some time, similar to the orientation perpendicular to an

electric-field gradient. From these findings it is clear that cells are somehow able to test the flexibility of the substrate. One hypothesis is that the cells test mechanical substrate properties by applying increasing forces by a feedback loop where only a strong mechanical feedback leads to growing contact sites (Lo et al., 2000). This similar orientation response may indicate that the same mechanisms are involved in the reaction to electric fields and mechanosensing.

A mechanism for galvanotaxis could be due to separation of charged components of the plasmatic membrane by electrophoresis (Jaffe, 1977). Accumulation of receptors at the cathode-facing margins has been shown in various experiments (Poo et al., 1979; Fang et al., 1999). This theory can be used to explain the perpendicular elongation of cells that require a certain self-induced cytoskeletal tension along the axis they are elongating to. If all free integrins linking the cytoskeleton and the extracellular matrix drift towards an electrode and accumulate there, then the cell would only be able to connect two focal adhesions and increase tension between them if they are on an axis perpendicular to the drift. As all cellular interactions are highly dynamic, it is just a question of time until disassembly of focal contacts on the opposite side of the drift destination leads to another drift. By this mechanism the cell is then no longer able to maintain protrusions with the same orientation as the electric field. Although this hypothesis can be used to explain retraction, elongation and migration, it cannot explain why the traction forces increase prior to the visible retraction.

How the cells sense weak electric fields remains a difficult problem. The simplest hypothesis would be that the electric field is applying mechanical forces directly to the cell. However the force changes we visualize do not support this hypothesis, the initial force changes act inwards. Traction

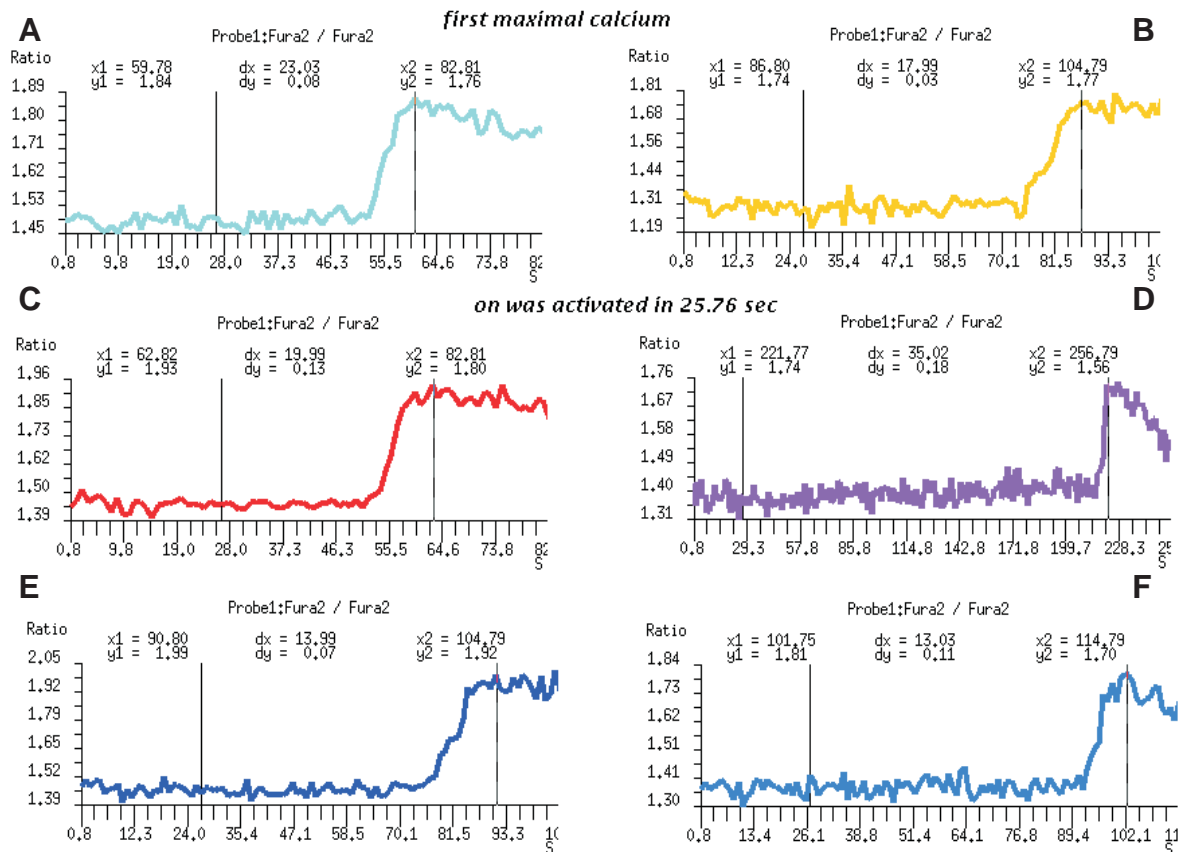


**Fig. 9.** Screen shot showing intracellular free-calcium measurement of 6 cells (A-F) exposed to a 10-V/cm electric field. The field was applied at 25.76 seconds (first bar). Times for the onset of calcium rise were 34 seconds for A, 61 seconds for B, 37 seconds for C, 196 seconds for D, 65 seconds for E and 76 seconds for F.

vectors caused by the field at facing margins perpendicular to the electric field show opposing directions.

One effect that can induce forces if the electric field causes polarization of the membrane is the so-called converse flexoelectricity (Petrov et al., 1993). The lipid bilayer of cell membranes contains charged proteins, which repel each other, influencing tension within the membrane. If the charge on one side of the membrane is changed, the membrane tension also changes. An acting force rebalances the surface tension of both sides of the membrane. This results in a changed curvature of the membrane. Flexo-electric effects of voltage-clamped HEK293 have been measured with an atomic force microscope (Zhang et al., 2001). Although flexo-electric effects can potentially explain a stimulation of the cell, these forces are probably not sufficient to cause the effects we measured.

Our results show that before any movement occurs, cell tensions change in a pattern related to the direction of the stimulus and also to the direction of future cell movement. This increase in cell tension might appear before the change of intracellular free calcium levels. There might therefore be more than one mechanism present in the cell that senses electric fields. One possibility is that one process causes the retraction and then the cell compensates the reduced cell-spreading area by re-spreading (Chen, 1979; Dunn and Zicha, 1995), whereas another mechanism could cause the cell to spread only perpendicular to the electric field. Electrophoretical drift of membrane proteins and the durotaxis phenomenon are possible

theories for explaining this directional re-spreading. Our measurements were made with a high-resolution integrating camera that was unable to gather images faster than 10 seconds. To measure the dynamics of the development of the contraction process we will need to use a high resolution intensified camera, which are only just becoming available. A method for simultaneously analyzing traction force and  $\text{Ca}^{2+}$  concentration at low resolution is now published (Doyle and Lee, 2002). However, we have not been able to measure  $\text{Ca}^{2+}$  concentrations and force together at high resolution as our methodology cannot achieve the necessary resolution for the traction-force calculation. Some modification of our equipment will be necessary to achieve this. Ultimately this will help to resolve the mechanism of electric field sensing by cells.

This work was supported by a grant from the Deutsche Luft und Raumfahrt (German Space Agency) DLR 50WB 9921 to D.B.J. and a NIH grant RO1 GM 61806 to M.D. M.M. was supported by a scholarship from Conacyt (Mexico) grant number 65369/116790.

## References

- Bereiter-Hahn, J. and Luers, H. (1998). Subcellular tension fields and mechanical resistance of the lamella front related to the direction of locomotion. *Cell Biochem. Biophys.* **29**, 243-262.
- Billiau, A., Edy, V. G., Heremans, H., van Damme, J., Desmyter, J., Georgiades, J. A. and de Somer, P. (1977). Human interferon: mass production in a newly established cell line, MG-63. *Antimicrob. Agents Chemother.* **12**, 11-15.



- Brighton, C. T., Adler, S., Black, J., Itada, N. and Friedenberg, Z. B. (1975). Cathodic oxygen consumption and electrically induced osteogenesis. *Clin. Orthop.* **107**, 277-282.
- Brown, M. J. and Loew, L. M. (1994). Electric field-directed fibroblast locomotion involves cell surface molecular reorganization and is calcium independent. *J. Cell Biol.* **127**, 117-128.
- Burton, K., Park, J. H. and Taylor, D. L. (1999). Keratocytes generate traction forces in two phases. *Mol. Biol. Cell* **10**, 3745-3769.
- Chen, W. T. (1979). Induction of spreading during fibroblast movement. *J. Cell Biol.* **81**, 684-691.
- Collinsworth, A. M., Torgan, C. E., Nagda, S. N., Rajalingam, R. J., Kraus, W. E. and Truskey, G. A. (2000). Orientation and length of mammalian skeletal myocytes in response to a unidirectional stretch. *Cell Tissue Res.* **302**, 243-251.
- Cooper, M. S. and Keller, R. E. (1984). Perpendicular orientation and directional migration of amphibian neural crest cells in dc electrical fields. *Proc. Natl. Acad. Sci. USA* **81**, 160-164.
- Cooper, M. S. and Schliwa, M. (1985). Electrical and ionic controls of tissue cell locomotion in DC electric fields. *J. Neurosci. Res.* **13**, 223-244.
- Crowley, E. and Horwitz, A. F. (1995). Tyrosine phosphorylation and cytoskeletal tension regulate the release of fibroblast adhesions. *J. Cell Biol.* **131**, 525-537.
- Dembo, M., Oliver, T., Ishihara, A. and Jacobson, K. (1996). Imaging the traction stresses exerted by locomoting cells with the elastic substratum method. *Biophys. J.* **70**, 2008-2022.
- Dembo, M. and Wang, Y. L. (1999). Stresses at the cell-to-substrate interface during locomotion of fibroblasts. *Biophys. J.* **76**, 2307-2316.
- Djamgoz, M. B. A., Mycielska, M., Madeja, Z., Fraser, S. P. and Korohoda, W. (2001). Directional movement of rat prostate cancer cells in direct-current electric field: involvement of voltage gated Na<sup>+</sup> channel activity. *J. Cell Sci.* **114**, 2697-2705.
- Doyle, A. D. and Lee, J. (2002). Simultaneous, real-time imaging of intracellular calcium and cellular traction force production. *Biotechniques* **33**, 358-364.
- Dunn, G. A. and Zicha, D. (1995). Dynamics of fibroblast spreading. *J. Cell Sci.* **108**, 1239-1249.
- Fang, K. S., Ionides, E., Oster, G., Nuccitelli, R. and Isseroff, R. R. (1999). Epidermal growth factor receptor relocalization and kinase activity are necessary for directional migration of keratinocytes in DC electric fields. *J. Cell Sci.* **112**, 1967-1978.
- Forscher, P. (1989). Calcium and polyphosphoinositide control of cytoskeletal dynamics. *Trends Neurosci.* **12**, 468-474.
- Glogauer, M., Arora, P., Yao, G., Sokholov, I., Ferrier, J. and McCulloch, C. A. (1997). Calcium ions and tyrosine phosphorylation interact coordinately with actin to regulate cytoprotective responses to stretching. *J. Cell Sci.* **110**, 11-21.
- Grynkiewicz, G., Poenie, M. and Tsien, R. Y. (1985). A new generation of Ca<sup>2+</sup> indicators with greatly improved fluorescence properties. *J. Biol. Chem.* **260**, 3440-3450.
- Harris, A. K., Pryer, N. K. and Paydarfar, D. (1990). Effects of electric fields on fibroblast contractility and cytoskeleton. *J. Exp. Zool.* **253**, 163-176.
- Jaffe, L. F. (1977). Electrophoresis along cell membranes. *Nature* **265**, 600-602.
- Jay, P. Y., Pham, P. A., Wong, S. A. and Elson, E. L. (1995). A mechanical function of myosin II in cell motility. *J. Cell Sci.* **108**, 387-393.
- Jones, D. B. and Bingmann, D. (1991). How do osteoblasts respond to mechanical stimulation? *Cells and Methods* **1**, 329-340.
- Jones, D. B., Nolte, H., Scholubbers, J. G., Turner, E. and Veltel, D. (1991). Biochemical signal transduction of mechanical strain in osteoblast-like cells. *Biomaterials* **12**, 101-110.
- Jorgensen, T. E. (1972). The effect of electric current on the healing time of crural fractures. *Acta Orthop. Scand.* **43**, 421-437.
- Karl, I. and Bereiter-Hahn, J. (1999). Tension modulates cell surface motility: a scanning acoustic microscopy study. *Cell Motil. Cytoskeleton* **43**, 349-359.
- Lee, J., Ishihara, A., Oxford, G., Johnson, B. and Jacobson, K. (1999). Regulation of cell movement is mediated by stretch-activated calcium channels. *Nature* **400**, 382-386.
- Li, Y., Hu, Z. and Li, C. (1993). New method for measuring Poisson's ratio in polymer gels. *J. Appl. Polym. Sci.* **50**, 1107-1111.
- Lo, C. M., Wang, H. B., Dembo, M. and Wang, Y. L. (2000). Cell movement is guided by the rigidity of the substrate. *Biophys. J.* **79**, 144-152.
- Marganski, W. A., Dembo, M. and Wang, Y. L. (2003). Measurement of cell-generated deformations of flexible substrata using correlation-based optical flow. *Methods Enzymol.* **361**, 197-211.
- Moalli, M. R., Wang, S., Caldwell, N. J., Patil, P. V. and Maynard, C. R. (2001). Mechanical stimulation induces pp125(FAK) and pp60(src) activity in an in vivo model of trabecular bone formation. *J. Appl. Physiol.* **91**, 912-918.
- Munevar, S., Wang, Y. L. and Dembo, M. (2001). Traction force microscopy of migrating normal and H-ras transformed 3T3 fibroblasts. *Biophys. J.* **80**, 1744-1757.
- Neidlinger-Wilke, C., Grood, E. S., Wang, J. H. C., Brand, R. A. and Claes, L. (2001). Cell alignment is induced by cyclic changes in cell length: studies of cells grown in cyclically stretched substrates. *J. Orthop. Res.* **19**, 286-293.
- Nuccitelli, R. and Erickson, C. A. (1983). Embryonic cell motility can be guided by physiological electric fields. *Exp. Cell Res.* **147**, 195-201.
- Onuma, E. K. and Hui, S. W. (1988). Electric field-directed cell shape changes, displacement, and cytoskeletal reorganization are calcium dependent. *J. Cell Biol.* **106**, 2067-2075.
- Palmer, A. M., Messerli, M. A. and Robinson, K. R. (2000). Neuronal galvanotropism is independent of external Ca(2+) entry or internal Ca(2+) gradients. *J. Neurobiol.* **45**, 30-38.
- Petrov, A. G., Miller, B. A., Hristova, K. and Usherwood, P. N. (1993). Flexoelectric effects in model and native membranes containing ion channels. *Eur. Biophys. J.* **22**, 289-300.
- Poo, M., Lam, J. W., Orida, N. and Chao, A. W. (1979). Electrophoresis and diffusion in the plane of the cell membrane. *Biophys. J.* **26**, 1-21.
- Radmacher, M., Tillmann, R. W., Fritz, M. and Gaub, H. E. (1992). From molecules to cells: imaging soft samples with the atomic force microscope. *Science* **257**, 1900-1905.
- Rees, D. A., Charlton, J., Ataliotis, P., Woods, A., Stones, A. J. and Bayley, S. A. (1989). Myosin regulation and calcium transients in fibroblast shape change, attachment, and patching. *Cell Motil. Cytoskeleton* **13**, 112-122.
- Sheetz, M. P., Felsenfeld, D. P. and Galbraith, C. G. (1998). Cell migration: regulation of force on extracellular-matrix-integrin complexes. *Trends Cell Biol.* **8**, 51-54.
- Steckel, R. R., Page, E. H., Geddes, L. A. and van Vleet, J. F. (1984). Electrical stimulation on skin wound healing in the horse: preliminary studies. *Am. J. Vet. Res.* **45**, 800-803.
- Stewart, R., Erskine, L. and McCaig, C. D. (1995). Calcium channel subtypes and intracellular calcium stores modulate electric field-stimulated and -oriented nerve growth. *Dev. Biol.* **171**, 340-351.
- Strohmeier, R. and Bereiter-Hahn, J. (1984). Control of cell shape and locomotion by external calcium. *Exp. Cell Res.* **154**, 412-420.
- Struckmeier, J., Klopp, E., Born, M., Hofmann, M., Rink, D., Jones, D. B. and Butt, H. (2001). Real-time atomic force fluorescence microscopy on living cells. *Proc. SPIE The International Society for optical engineering* **4434**, 142-149.
- Wang, H. B., Dembo, M., Hanks, S. K. and Wang, Y. L. (2001). Focal adhesion kinase is involved in mechanosensing during fibroblast migration. *Proc. Natl. Acad. Sci. USA* **98**, 11295-11300.
- Wang, Y. L. and Pelham, R. J. Jr (1998). Preparation of a flexible, porous polyacrylamide substrate for mechanical studies of cultured cells. *Methods Enzymol.* **298**, 489-496.
- Zhang, P. C., Keleshian, A. M. and Sachs, F. (2001). Voltage-induced membrane movement. *Nature* **413**, 428-432.